

Chapter 3

Flight Operations

3.1 Overview

3.1.1 Mission Overview

COBE was launched aboard Delta rocket No. 189 at 1434 UT on 1989 November 18 from the Western Space and Missile Center at the Vandenberg Air Force Base in California into the desired orbit. The spacecraft and orbital characteristics are given in Table 3.1-1.

Table 3.1-1: *COBE* spacecraft and orbital characteristics

Orbit	
Altitude at insertion	900.2 km
Inclination	99°3
Eccentricity at launch	0.0006
Mean eccentricity over 1 yr	0.0012
Time of ascending node	6 pm
Dimensions of spacecraft	
Total mass	2270 kg
Length	5.49 m
Diameter	8.53 m (with solar panels deployed) 2.44 m (with solar panels folded at launch)
Orbital period	103 minutes (nominal)
Spacecraft rotation rate	0.8 rpm (nominal)
Power available	750 W
Data rate	4 kbps
Dewar	
Capacity available	650 liters
At launch:	
Fill	100%
Fill after pump down	92.7%
Internal temperature	1.7 K
In orbit:	
Internal temperature	1.4 K
Sun-Earth shield inner side temperature	180 K
Lifetime of helium in orbit	307 days

The dewar cover was ejected three days after launch, and the *DIRBE* instrument began to collect science data on the same day. During the first month in orbit, various tests were undertaken to evaluate the performance of the instruments and spacecraft, and to optimize instrument parameters.

All of the spacecraft systems operated well, allowing the mission design requirements to be achieved. According to plan, the satellite spin rate was increased in several small steps (see Table C.0-1) from an initial rate of ~ 0.23 rpm, and the nominal 0.8 rpm spin rate was attained 9 days after launch. One of *COBE*'s transverse control axis gyros failed electrically on the fourth day after launch. However, because of redundancy built into the attitude control system, normal operations continued. The remaining gyros and all other spacecraft systems performed flawlessly during the lifetime of the cryogen. On 1991 September 7, one of the three gyros on the spin axis failed, and, once again, no data were lost. Fine aspect solutions were not carried out for three days while operational changes were made.

The spacecraft altitude decreased at the rate of 30 m per day during the first 10 months of flight, due largely to the thrust from the effluent helium. (The tilt-back of the spacecraft from the velocity vector described in §2.3.3 caused the venting helium to apply a small force opposite to the velocity.) This altitude loss did not pose a problem but had to be considered in the attitude reconstruction.

COBE operated in a routine survey mode. During the cryogenic lifetime, the satellite was periodically tilted a few degrees further away from the Sun than the nominal 94° . This maneuver was carried out at the beginning and end of each *FIRAS* calibration to ensure that the *FIRAS* external calibrator would not be exposed to direct sunlight.

The dewar performed thermally better than expected. In flight, the helium temperature inside the main cryogen tank was 1.40 K (the design requirement was 1.6 K). The temperature of the inner surface of the Sun–Earth shield was 180 K (the requirement was 220 K), allowing the outer dewar wall and cryogenic instruments to operate at colder temperatures. As expected, the Earth limb rose a few degrees above the Sun–Earth shield for a part of every orbit during a three month period starting in May. During this period (referred to as “eclipse season” for reasons described in §2.3.3), the Earth’s radiation produced thermal transients in the instruments and adversely affected data for a portion of each orbit. Some of these data were still usable after careful calibration (see §4.7.7). The 10–month lifetime of the cryogen is consistent with the detailed pre–launch model of the cryostat after taking into account Earth limb heating near the summer solstice, anomalous behavior in the *FIRAS* mirror transport mechanism (see §3.5.3.1), and the heat dissipated in normal operation and calibration cycles of the instruments.

The three instruments completed their first full sky coverage by mid–June 1990, and returned high quality data until the liquid helium ran out at 0936 UT on 1990 September 21. Once the cryogen was gone, the six longest wavelength bands of the *DIRBE* were turned off; data acquisition (including polarimetry) continued at 1.25, 2.2, 3.5 and 4.9 μm , albeit at reduced sensitivity. Near–infrared sky maps of the large scale interplanetary dust signals continued to be of adequate quality to permit searching for evidence of temporal changes on annual time scales over a 4 yr period until all *COBE* operations were finally discontinued on 1993 December 23.

3.1.2 *DIRBE* Sky Coverage

DIRBE's helical scans (see §2.3.4) covered the sky nonuniformly. Portions of the sky that were observed at the solar elongation extrema ($\epsilon \sim 94^\circ \pm 30^\circ$) were scanned more frequently than regions that lay closer to the center of the viewing swath (at $\epsilon \sim 94^\circ$). Furthermore, unlike directions within $\sim 30^\circ$ of the ecliptic poles, which were observed year–round, sites along the ecliptic plane were in range for 2 months and then remained inaccessible for 4 months before coming back into view.

Figure 3.1-1 shows the depth of coverage attained (after rejection of low–quality data; see §4.7) during a typical week and for the entire cryogenic mission (10 months). In a week, a typical pixel was observed ~ 10 – 15 times, and the most densely–surveyed pixels, which delineate two circumpolar annuli at ecliptic latitudes, $|\beta| \simeq 60^\circ$, were observed ~ 80 – 100 times. Over the course of the cryogenic mission, most pixels were observed approximately 200 times, those at $|\beta| \simeq 60^\circ$ were observed ~ 800 – 1000 times, and those at the ecliptic polar caps ($|\beta| > 60^\circ$) were observed roughly 400–500 times. Because the cryogenic mission lasted for 10 months rather than a full year, coverage along the ecliptic equator is also uneven. The coverage was relatively sparse at ecliptic longitudes near 120° and 300° .

Table 3.1-2 lists a range of solar elongation angles and two ranges of ecliptic longitudes spanned by the *DIRBE* scan path at the ecliptic equator for each week of the cryogenic mission. Two ecliptic longitude ranges are given. Those denoted “Ascending” refer to ecliptic plane crossings from South to North;

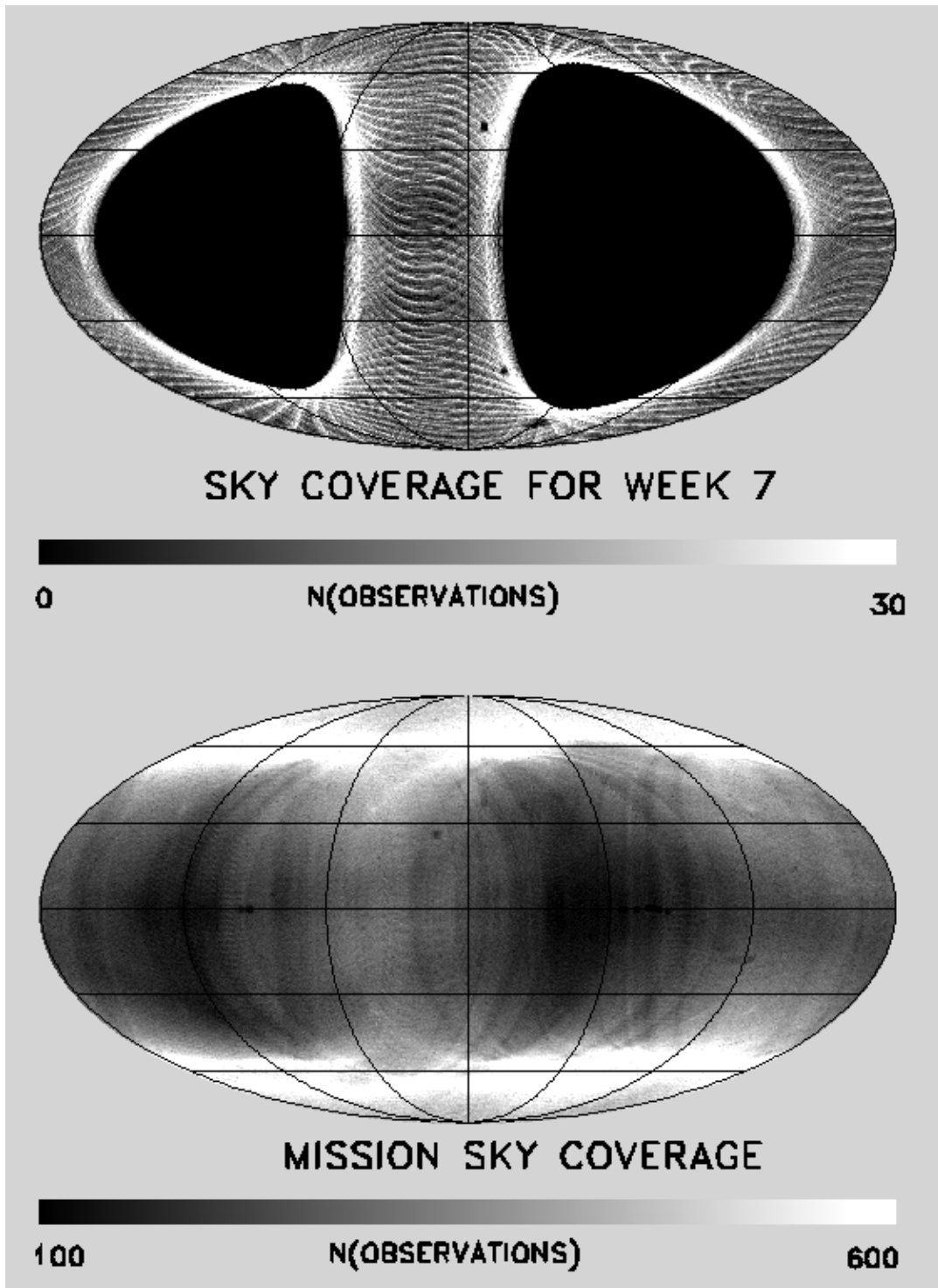


Figure 3.1-1: Number of observations per pixel for (a) week 7 and (b) the entire cryogenic mission. The maps are ecliptic coordinate projections.

Table 3.1-2: Weekly sky coverage

File	Week	Time interval (yyddd)	Elongation range (°)	Ecliptic longitude range (°)	
				Ascending	Descending
1	4	89345 – 89351	63 – 125	323 – 29	201 – 132
2	5	89352 – 89358	63 – 128	329 – 38	209 – 138
3	6	89359 – 89365	65 – 124	338 – 44	216 – 149
4	7	90001 – 90007	65 – 124	346 – 50	223 – 156
5	8	90008 – 90014	65 – 124	353 – 59	230 – 163
6	9	90015 – 90021	65 – 128	0 – 68	237 – 170
7	10	90022 – 90028	65 – 124	7 – 73	244 – 178
8	11	90029 – 90035	65 – 124	14 – 80	251 – 185
9	12	90036 – 90042	65 – 124	21 – 87	258 – 192
10	13	90043 – 90049	65 – 128	28 – 98	265 – 199
11	14	90050 – 90056	65 – 124	35 – 101	272 – 206
12	15	90057 – 90063	65 – 124	42 – 109	277 – 213
13	16	90064 – 90070	65 – 124	49 – 116	286 – 220
14	17	90071 – 90077	65 – 126	56 – 124	292 – 227
15	18	90078 – 90084	65 – 124	63 – 129	295 – 234
16	19	90085 – 90091	62 – 124	69 – 136	305 – 241
17	20	90092 – 90098	65 – 124	77 – 143	314 – 248
18	21	90099 – 90105	65 – 124	84 – 150	321 – 255
19	22	90106 – 90112	63 – 128	94 – 156	330 – 259
20	23	90113 – 90119	63 – 122	99 – 161	337 – 271
21	24	90120 – 90126 ^a	62 – 122	102 – 168	344 – 278
22	25	90127 – 90133	62 – 122	109 – 175	350 – 286
23	26	90134 – 90140	62 – 128	116 – 183	356 – 286
24	27	90141 – 90147	64 – 123	124 – 189	2 – 297
25	28	90148 – 90154	63 – 122	132 – 194	10 – 303
26	29	90155 – 90161	63 – 122	136 – 202	17 – 311
27	30	90162 – 90168	63 – 122	143 – 208	23 – 318
28	31	90169 – 90175	63 – 122	149 – 215	30 – 324
29	32	90176 – 90182	63 – 124	156 – 223	37 – 329
30	33	90183 – 90189	63 – 122	163 – 228	44 – 338
31	34	90190 – 90196	63 – 122	169 – 235	50 – 344
32	35	90197 – 90203	63 – 126	176 – 246	57 – 351
33	36	90204 – 90210	63 – 122	183 – 249	64 – 358
34	37	90211 – 90217	63 – 124	190 – 257	67 – 6
35	38	90218 – 90224	65 – 124	198 – 264	76 – 7
36	39	90225 – 90231 ^a	65 – 124	205 – 271	82 – 14
37	40	90232 – 90238 ^a	65 – 129	212 – 278	89 – 23
38	41	90239 – 90245	65 – 128	218 – 285	95 – 29
39	42	90246 – 90252	65 – 129	225 – 294	102 – 35
40	43	90253 – 90259	65 – 127	232 – 300	109 – 43
41	44	90260 – 90264	65 – 129	239 – 305	113 – 50

^a coverage reduced due to JFET-off test.

“Descending” scans cross the ecliptic plane from North to South. To first order, the elongation range was constant ($64^\circ \leq \varepsilon \leq 124^\circ$). However, small perturbations in elongation coverage were introduced during the eclipse season (see §2.3.3) and during roll maneuvers (see §3.1.1), and the coverage was extremely sparse during JFET-off test periods (see §3.3.2).

3.2 DIRBE Operations

3.2.1 Launch to End of Cryogen

During the three-week period following launch the *DIRBE* instrument’s functionality was verified and the operating parameters were optimized. The instrument was found to be operating normally, except for the 100 μm annealing heater, which had failed prior to launch (see §3.5.1). As expected, the initial detector operating parameters chosen on the basis of ground tests were not ideally-suited to operation in space. Thus, although the sky was observed, data obtained during the verification period are of limited scientific value. By 1989 November 28 the dewar had stabilized and optimization tests were begun. The objective of these tests was to find detector bias settings, static heater levels, multiplexor (MUX) sampling positions, commandable gains, etc. that provided the highest signal-to-noise ratio for sky signals, and yet maintained detector linearity.

Table 3.2-1: Nominal detector operating parameters: cryogenic era

Detector	MUX position ^a	Data delay ^a	Bias ^b (V)	Heater ^b (V)	Commanded ^c gain	DC ^d	DGL ^e
1A	6	5	.149	.498	G1 (3)	IN	OFF
1B	7	5	.149	.498	G1 (3)	IN	OFF
1C	5	5	.149	.498	G1 (3)	IN	OFF
2A	10	5	.149	.498	G1 (3)	IN	OFF
2B	16	5	.149	.498	G1 (3)	IN	OFF
2C	1	6	.149	.498	G1 (3)	IN	OFF
3A	9	5	.149	.498	G1 (3)	IN	OFF
3B	13	5	.149	.498	G1 (3)	IN	OFF
3C	14	5	.149	.498	G1 (3)	IN	OFF
4	11	1	.149	.498	G1 (3)	IN	OFF
5	3	5	1.103	.23	G0 (1)	IN	OFF
6	15	5	1.103	.23	G0 (1)	IN	OFF
7	2	1	.24	.192	G0 (1)	IN	OFF
8	8	1	.24	broken	G0 (1)	IN	OFF
9	4	4	2.682	N/A	G1 (3)	IN	OFF
10	12	4	1.907	N/A	G1 (3)	IN	OFF

^a Settings result in optimal phasing of science data samples with respect to chopper cycle at nominal operating temperature (see §2.2.6).

^b Settings optimize detector linearity and signal-to-noise at nominal operating temperature. The quoted heater settings are those used during normal science data mode, not during thermal annealing (see §2.2.2).

^c Analog gain chosen to maximize dynamic range in the digitized data without saturating in sky or calibration modes (see §§2.2.5 and 3.3.2.3).

^d IN indicates “DC offset injected.”

^e With on-board deglitching (DGL) activated (ON), the microprocessor would reject high and low chopper cycle samples and average the remaining two samples to yield an SDM datum; with DGL OFF, all four chopper cycle samples were combined into an SDM datum.

Routine survey work commenced on 1989 December 11 at 01:04 UT, when the *DIRBE* was configured with the final detector operating parameters chosen for the cryogenic mission (Table 3.2-1). The strategy

ultimately adopted to compensate for the failure of the 100 μm annealing heater (see §3.5.1) was implemented on 1990 January 1. Until then, a variety of annealing “recipes” were tested (see §3.5.1).

Aside from the routine characterization and monitoring tests discussed in §3.3, the *DIRBE* configuration remained stable for the rest of the cryogenic mission, with two exceptions. The first was a test conducted between 1989 December 29 03:22 UT and 1989 December 30 01:57 UT, in which the bias voltage on the 60 μm detector was temporarily changed in order to examine the effect of bias voltage on noise. After the test, the voltage was reset to the value shown in Table 3.2-1. The second configuration change was designed to reduce the lunar-induced noise described in §4.7.5 and involved powering off the band 1B (1.25 μm) detector twice a month when the Moon came into view. That change was initiated on 1990 August 29. Various possible noise suppression procedures were tested during the period from 1990 July 10 to 16 (see Appendix C). The procedure finally adopted involved reactivating the band 1B detector about 6 days after it was turned off, when the Moon was no longer visible.

3.2.2 End of Cryogen to End of Mission

Following cryogen depletion, the 1.25, 2.2, 3.5, and 4.9 μm detectors continued to operate with sensitivity decreased by about an order of magnitude (largely due to the decrease in load resistance). By November 1991, 14 months into the “warm era,” the temperature at the *DIRBE* detectors had climbed to about 50 K. Useful data were obtained over a period that lasted until December 1993. The *DIRBE* warm-era data, which have potential to aid in modeling the zodiacal dust, in particular its evolution and dynamics, may prove useful in the search for the CIB.

3.3 *DIRBE* Characterization and Monitoring Tests

On-orbit operations were tailored to produce as much survey data as possible while retaining full knowledge of the performance of the instrument. Some instrument characterization procedures were followed regularly each day while others were carried out occasionally as deemed necessary.

3.3.1 Daily Events

The procedures described in Table 3.3-1 were repeated throughout the mission, allowing the system gains and offsets to be monitored as a function of time. To determine electrical and radiative offsets the instrument signal was measured with the shutter closed and the internal reference source (IRS) off. Then the IRS was turned on at various fixed levels to check the system gain. Following each calibration sequence, the *DIRBE* was commanded over to the survey mode and the shutter was opened.

The basic calibration sequence (“IRS run”) shown in the first row of Table 3.3-1 was performed about six times per orbit.¹ Because of the destabilizing effects on detectors of the intense ionizing radiation present in the South Atlantic Anomaly, calibration runs were conducted upon entering and exiting the SAA. The detectors were annealed after each SAA crossing prior to the IRS run. Accounting for routine interruptions, survey data were obtained approximately 82% of the time, yielding 560,000 $\frac{1}{8}$ -second science mode samples per day.

3.3.2 Special On-orbit Tests

In addition to the daily calibration activities, special on-orbit tests were conducted to monitor detector linearity, contributions to the instrumental offsets from heat produced by the JFET amplifiers, and stability of the analog commandable gain.

¹Upon entering and exiting the Van Allen belt surrounding the North magnetic pole (NVAB); upon entering and exiting the Van Allen belt surrounding the South magnetic pole (SVAB); upon entering and exiting the South Atlantic Anomaly (SAA); and at a random time in the first and second halves of each day.

Table 3.3-1: Non-survey daily operations

Purpose	Frequency (times/day)	Procedure
Basic calibration sequence <ul style="list-style-type: none"> • Measure detector offsets in science data mode (SDM); and • Measure relative detector gain 	~ 75	<ul style="list-style-type: none"> • Close the shutter and observe the dark response of the detectors for 32 seconds; and • Operate one of the IRS sources under an on-board source-driving program.^a Following IRS exposure, keep the shutter closed and check for normal detector recovery.
Measure detector response to redundant Internal Reference Sources in case the primary IRS fails	~ 2	Make back-to-back observations ^a of the sources designated “primary” and “secondary” at least once per day; make additional observations of all four calibration sources back-to-back once per day, either upon exiting the Van Allen belt surrounding the North magnetic pole (NVAB) or upon entering the southern Van Allen belt (SVAB). The primary/secondary source measurements were made more frequently (at every NVAB exit) after 1990 July 7.
Anneal detectors to remove effects of SAA passage	~ 11	Heat 60 μm detector to ~ 20 K and simultaneously flood detectors with radiation from a backup IRS bright enough to saturate 60 and 100 μm detectors.
Measure detector offsets and evaluate noise in SNAP mode (see §2.2.6)	~ 1	Observe shutter-closed dark response for every detector at $2\times$ the synchronous demodulation sampling rate ^b

^a In the standard program the source voltage was ramped up in staircase fashion: the voltage was incremented by a known amount, held constant for 2 seconds, and then incremented again. The process was repeated 32 times.

^b These data also provide information on the electronics transfer function, since the response to a charged-particle-induced delta function input is seen occasionally.

3.3.2.1 Linearity Tests

Interlocked IRS tests involved closing the shutter, running a reference source (IRS) through an illumination sequence (step ramp), pausing, running a second IRS through a similar sequence, and then running both sources through the sequence together, with one sequence starting later than the other. Linearity was measured at various levels of illumination by comparing the response of the detectors to the individual sources to the response to the summed intensity.

“Shutter flutter” tests involved closing and opening the shutter at several-second intervals while the IRS was on, thus exposing the detectors alternately to an IRS and the sky. These tests measured the time required for the detectors to stabilize following a change in the level of illumination, as well as the linearity in recovery following exposure to a variety of intensities. The Mission Events Log in Appendix C shows when these tests were conducted.

Absolute differential linearity tests were designed to determine the response of the detectors to an impulse of fixed brightness seen against various background brightness levels. An IRS staircase ramp sequence was run in which the source voltage was increased by a known increment, held fixed for 32 seconds, and then incremented again to form the background. A second IRS source was activated during each background step for 12 seconds at a fixed voltage.

3.3.2.2 JFET-off Test

Normally the JFET amplifiers, which are components of the preamplifiers of all the detectors, are on at all times. Although the JFETs are thermally isolated from the detectors, their thermal radiation could be injected “upstream” of the chopper, modulated, and appear as a component of the 32 Hz signal at the detectors. JFET thermal radiation was detectable at long wavelengths.

A “JFET-off” test was designed to measure the radiative contribution to the detector offsets attributable to the JFETs. The test sequence took a week to execute and consisted of the following steps:

Day 1: Turn off JFETs for bands 1–6; take data in bands 7–10;

Day 2: additionally turn off band 7 JFET; take data in bands 8–10;

Day 3: additionally turn off band 8 JFET; take data in bands 9 and 10;

Days 4–6: continue data collection in bands 9 and 10;

Day 7: activate JFETs in groups of detectors in the following sequence: bands 4–8, bands 1–3 A and B channels, bands 1–3 C channels.

Normal daily operations continued during the test, except that special monitoring was done with the shutter closed while the JFETs cooled. The JFETs for bands 9 and 10 were not turned off because detector assembly no. 3, which held the 140 and 240 μm detectors, was enclosed in a light-tight environment; these JFETs had no potential to affect any of the detectors.

Two JFET-off tests were performed during the cryogenic mission, one that lasted from 1990 April 30 – May 6 (90120 – 90126), and another from 1990 August 15 – 21 (90227 – 90233). Relatively little science data was obtained during these periods.

3.3.2.3 Analog Gain

The relative values of the analog commandable gains were measured prior to launch. Gain stability was checked five times on-orbit during the cryogenic period by closing the shutter and feeding square wave electrical test signals of various amplitudes directly into the analog signal processing electronics. The detectors were bypassed, but the signal propagated through the rest of the electronics as if it had been observed by the detectors.

3.4 Anticipated Environmental Influences

3.4.1 Nuclear Radiation Effects on Detectors

The effects of ionizing radiation on the detectors were anticipated before launch. Ground tests in proton beams showed that the Ge:Ga detectors became noisier and changed in responsivity when exposed to ionizing radiation doses comparable to the expected one-pass SAA dose.

In flight, there were both short and long term effects. When ionizing particle hits were infrequent, the interactions caused transient events (“glitches”) in the detectors which were recognized by their short duration (shorter than the passage of a point source) and removed from the data stream in the ground data processing. When particle hit rates were very high, such as in the SAA, the data were corrupted and unsalvageable (see §4.7, in which Figure 4.7-1 shows the 100 μm glitch frequency as a function of satellite position over the surface of the Earth).

Some of the detectors, particularly the Ge:Ga photoconductors (60 and 100 μm bands), did not return to nominal operating condition for a long time after exposure to a high dose of ionizing radiation. An overbiasing technique intended to improve detector stability was used on the Infrared Astronomical Satellite (*IRAS*; Neugebauer *et al.* 1984), but the technique was only modestly successful. Prelaunch tests on the *DIRBE* Ge:Ga detectors showed that elevating the temperature of the detectors would produce a much more rapid and reliable return to stable operating conditions. A small resistive heater was attached to a thermally isolated detector mount under each *DIRBE* detector to control the operating temperature and permit thermal annealing for the effects of radiation. Command sequences were developed to provide the short term heating required to anneal the detectors and restore them to nominal operating conditions. Unfortunately, the 100 μm heater was found to be defective late in ground testing, and a modified annealing procedure had to be implemented (see §3.5.1).

3.4.2 Photon-induced Responsivity Enhancement

“Photon-induced responsivity enhancement” (PIRE) refers to the effect of *previous* illumination on a detector’s current response to incident light. PIRE was detected and its magnitude estimated by taking advantage of the fact that the photometric history of the instrument before it observed each pixel depended upon the approach direction; the difference in brightness measured at a pixel when it was approached from different scan directions was used to estimate the size of the enhancement. The magnitude of the PIRE effect reached 30–40% at 100 μm and about 5% at 60 μm near the brightest parts of the Galactic plane; the effect was very small (less than a few percent in individual observations) at other wavelengths. Corrections made to mitigate the effect at 100 μm and residual errors will be discussed in Chapter 4.

3.4.3 Thermal Changes Within the Dewar

The temperature within the *COBE* dewar varied during the mission as a result of both external and internal influences (*e.g.*, solar eclipses, changes in the instrument operating mode, anomalous behavior of the *FIRAS* mirror transport mechanism). The temperature was monitored at a rate of one reading per 32 seconds by 15 Germanium Resistance Thermometers (GRTs) mounted at various places on the *DIRBE* optical module. There were two GRTs on each of the three detector assemblies. The detector temperature data were used to correct for thermally induced gain variations (see §4.5.3). Thermal effects were further suppressed by disregarding the data obtained with a detector when its temperature exceeded a detector-dependent threshold value (see §4.7.7). Because these measures were taken, the residual errors in the data products due to temperature variations are negligible.

3.4.4 Thermal Changes External to the Dewar

With the onset of eclipse season (see §2.3.3) in May 1990, the temperature of the *DIRBE* warm electronics (external to the dewar) began dropping from a nominal value of ~ 21 °C to a minimum of ~ 16 °C at longest eclipse duration. The chopper drive electronics were temperature sensitive and the chopper phase changed as the temperature changed. Depending upon a detector’s sampling position within the

MUX (see §2.2.6 and Table 3.2-1), the detector responsivity was either enhanced or depressed as the chopper phase changed. Smooth, long-term responsivity variations due to this effect were calibrated out through the use of celestial standards (see §4.5).

3.4.5 Atmospheric Glow

Constituents of the Earth’s atmosphere at *COBE*’s orbital altitude can be induced to glow by collisions with the spacecraft. Neutral atomic oxygen, for example, has emission lines at 63 and 147 μm . The telltale sign of atmospheric glow is brighter emission in the forward ram direction.

Like PIRE, evidence for atmospheric glow was sought by comparing observations of selected celestial directions made from opposite “approach vectors” along the *DIRBE* scan path, taking advantage of the fact that many pixels approached from one direction were approached and reobserved a short time later from a different direction. The approach vectors are denoted AV1 and AV2, the former vector having a component in the direction of spacecraft motion in which atmospheric glow emission, if present, would have been brighter.

Isolation of atmospheric glow effects from others that contributed to approach vector differences proved difficult. Neither visual inspection of AV1 – AV2 maps nor detailed studies of selected patches of the sky yielded convincing evidence of atmospheric effects distinguishable from residual PIRE, IRS–induced gain changes, or beam offset effects in any photometric band.

3.5 *DIRBE* Malfunctions and *COBE* Influences

3.5.1 Band 8 Annealing Heater

Shortly before launch the 100 μm (band 8) annealing heater was found to have failed. It was too late to repair the problem. Tests were conducted in flight between 1989 December 11 and 1990 January 1 in order to devise a new annealing strategy. Various combinations and durations of overbiasing and illumination with the internal calibration sources were considered. The annealing procedure adopted on 1990 January 1 consisted of exposing the focal plane to intense light from an IRS for 100 s. The 100 μm data obtained prior to 1990 January 1 are of lower quality than the data obtained later in the mission. A particularly ineffective annealing procedure was used during 1989 December 12 – 17; the band 8 data obtained during that period were excluded from the data products.

The 60 μm (band 7) annealing heater remained functional throughout the cryogenic mission. No other detectors were annealed with their heaters. An analysis of calibration data obtained prior to and following passage through the SAA indicated that response changes in the other detectors were no greater than 1% without heater annealing.

3.5.2 Primary IRS

Starting in May 1990 (around day 90135), the detectors began to register an increasing brightness from the primary IRS. This trend continued into the eclipse season, which started a couple of days later. Since the detector response to the secondary IRS, which had been monitored throughout the mission, remained constant, the anomalous behavior was attributed to the primary IRS. On 1990 July 7 (day 90188), the secondary IRS was substituted for the primary as the main internal reference source and thereafter monitored frequently. The original primary source continued to be monitored, but less frequently.

3.5.3 *FIRAS* Influences

Two *FIRAS* mechanisms occasionally influenced the performance of the *DIRBE*. According to detector temperature and signal-to-noise constraints described in §§4.7.7 and 4.7.5, respectively, the affected *DIRBE* observations were identified during data processing and excluded from the data products (see §§5.6.4 and 5.6.8).

3.5.3.1 *FIRAS* Mirror Transport Mechanism

Early in the mission, especially during passes through the SAA, the *FIRAS* mirror transport mechanism (MTM) driver electronics behaved anomalously and allowed the MTM to continue driving against one of its stops. The *DIRBE* detected these events as thermal spikes triggered by the anomalously high energy delivered to the dewar and as high frequency (microphonic) noise. The precise times of these events are given in the Mission Events Log (Appendix C). At other times the *FIRAS* MTM moved smoothly and was not detected by *DIRBE*. The anomalous behavior of the MTM was eliminated by operational changes instituted after 1990 March 20.

3.5.3.2 *FIRAS* External Calibrator

The *FIRAS* external calibrator (XCAL), a temperature-controlled precision blackbody source, was occasionally inserted into the mouth of the *FIRAS* antenna. *FIRAS* calibrations were performed throughout the mission with the XCAL set to different temperatures. These calibrations had two effects on the *DIRBE* instrument. First, the XCAL caused the *COBE* dewar temperature to rise. Second, microphonic noise was triggered by the motion of the XCAL. The microphonics affected *DIRBE* detector assembly 2 (bands 4–8), especially the 4.9 and 60 μm bands, and took ~ 75 s to subside after the XCAL was stowed.

